

## A Microfluidic Device with a Linear Temperature Gradient for Parallel and Combinatorial Measurements

Hanbin Mao, Tinglu Yang, and Paul S. Cremer\*

Contribution from the Department of Chemistry, Texas A & M University,  
College Station, Texas 77843

Received November 27, 2001

**Abstract:** Methods for obtaining combinatorial and array-based data as a function of temperature are needed in the chemical and biological sciences. It is presently quite difficult to employ temperature as a variable using standard wellplate formats simply because it is very inconvenient to keep each well at a distinct temperature. In microfluidics, however, the situation is very different due to the short length scales involved. In this article, it is shown how a simple linear temperature gradient can be generated across dozens of parallel microfluidic channels simultaneously. This result is exploited to rapidly obtain activation energies from catalytic reactions, melting point transitions from lipid membranes, and fluorescence quantum yield curves from semiconductor nanocrystal probes as a function of temperature. The methods developed here could be extended to protein crystallization, phase diagram measurements, chemical reaction optimization, or multivariable experiments.

### Introduction

The advent of parallel data acquisition and combinatorial techniques<sup>1</sup> has greatly expanded the experimental approaches employed in the biological and chemical sciences. Examples range from assays for genomics,<sup>2</sup> proteomics,<sup>3</sup> and small molecule screening<sup>4</sup> to materials synthesis<sup>5</sup> and catalyst optimization.<sup>6,7</sup> Typical strategies rely on arraying many compounds on a two-dimensional grid such as a DNA chip or a multiwell plate. Variables such as buffer conditions, chemical composition, and concentration can be easily controlled in a predetermined fashion at each address. Applying the additional variable of temperature to the combinatorial toolbox would be of great interest to all the fields mentioned above. Indeed, rapid optimization of chemical and biochemical synthesis as a function of temperature as well as the determination of phase transition temperatures and activation energies from single experiments could be directly incorporated into almost any high throughput strategy. Unfortunately, there are few methodologies now available for achieving these goals.<sup>8–10</sup> In fact, presently only a few distinct temperature measurements can be made in

wellplate formats by placing bulky independent temperature controllers under each segment.<sup>11</sup>

Herein we describe a very general approach using microfluidics<sup>12–14</sup> to generate a linear temperature gradient across a series of samples that can be quickly read off as a function of position. The principle we adopt for designing linear temperature control into an on-chip device<sup>15</sup> rests on the simple solution to the Fourier heat diffusion equation<sup>16</sup> when heat flow is restricted to one direction along a two-dimensional planar surface (eq 1).

$$\frac{d}{dx}\left(k\frac{dT}{dx}\right) = 0 \quad (1)$$

Here,  $T$  is temperature,  $x$  is the position variable along the direction of heat transfer, and  $k$  is the thermal conductivity of the medium in which the heat is flowing. If a hot reservoir and a cold sink are separated by a straight wall of thickness  $L$  within the plane, then eq 1 can be doubly integrated to show that the

\* To whom correspondence should be addressed. Tel: 979-862-1200. Fax: 979-845-7561. E-mail: cremer@mail.chem.tamu.edu.

- (1) Hanak, J. J. *J. Mater. Sci.* **1970**, *5*, 964.
- (2) Fodor, S. P. A.; Read, J. L.; Pirrung, M. C.; Stryer, L.; Lu, A. T.; Solas, D. *Science* **1991**, *251*, 767–773.
- (3) MacBeath, G.; Schreiber, S. L. *Science* **2000**, *289*, 1760–1763.
- (4) MacBeath, G.; Koehler, A. N.; Schreiber, S. L. *J. Am. Chem. Soc.* **1999**, *121*, 7967–7968.
- (5) Xiang, X. D.; Sun, X. D.; Briceno, G.; Lou, Y. L.; Wang, K. A.; Chang, H. Y.; Wallacefreedman, W. G.; Chen, S. W.; Schultz, P. G. *Science* **1995**, *268*, 1738–1740.
- (6) Taylor, S. J.; Morken, J. P. *Science* **1998**, *280*, 267–270.
- (7) Reddington, E.; Sapienza, A.; Gurau, B.; Viswanathan, R.; Sarangapani, S.; Smotkin, E. S.; Mallouk, T. E. *Science* **1998**, *280*, 1735–1737.
- (8) Thatcher, D. R.; Hodson, B. *Biochem. J.* **1981**, *197*, 105–109.
- (9) Rosenbaum, V.; Riesner, D. *Biophys. Chem.* **1987**, *26*, 235–246.

- (10) Wartell, R. M.; Hosseini, S. H.; Moran, C. P. *Nucleic Acids Res.* **1990**, *18*, 2699–2705.
- (11) For example, the 6-Position Independent Temperature Zone Block by J-KEM Scientific.
- (12) Harrison, D. J.; Fluri, K.; Seiler, K.; Fan, Z. H.; Effenhauser, C. S.; Manz, A. *Science* **1993**, *261*, 895–897.
- (13) Woolley, A. T.; Mathies, R. A. *Proc. Natl. Acad. Sci. U.S.A.* **1994**, *91*, 11348–11352.
- (14) Jacobson, S. C.; Hergenroder, R.; Koutny, L. B.; Ramsey, J. M. *Anal. Chem.* **1994**, *66*, 2369–2373.
- (15) Several on-chip temperature controllers have already been built in microfluidic devices using miniature heaters and Peltier cooling platforms. For example, on-chip polymerase chain reactions (PCR) in microfluidic devices have been demonstrated with various temperature controllers (see refs 37–39), thermocapillary pumping has been shown (see refs 40–41), and temperature measurements with dyes have been made (see ref 42).
- (16) Incropera, F. P.; DeWitt, D. P. *Fundamentals of Heat and Mass Transfer*, 3rd ed.; John Wiley & Sons: New York, 1990.

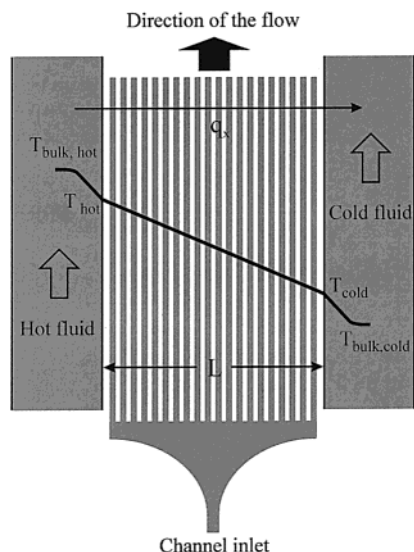


**Figure 1.** Illustration of the concept of a linear temperature gradient microfluidic system. The array of microfluidic channels sits between a hot source on the left and a cold sink on the right.  $q_x$  designates the direction of heat flow. The temperature varies linearly between the parallel heat source and sink where the portion of the device containing the linear array of microchannels is situated. Inside the heat source and sink the temperature gradient is nonlinear as heat is added and carried away, respectively.

temperature inside the wall varies linearly between the two interfaces (eq 2).

$$T(x) = T_{\text{cold}} + (T_{\text{hot}} - T_{\text{cold}})x/L \quad (2)$$

where  $T_{\text{cold}}$  is the temperature of the cold interface, and  $T_{\text{hot}}$  is the temperature of the hot interface (Figure 1). Although it is rather difficult to take practical advantage of this in the macroscopic world, the situation becomes much simpler inside a microfluidic device where heat exchange with the third dimension becomes negligible over the short length scales involved.

## Results

By branching a single microchannel into a series,<sup>17</sup> simultaneous measurements at different temperatures of otherwise chemically identical systems can be made as a simple function of position (Figure 2a). A plot of temperature versus position demonstrates the linearity of this device (Figure 2b).

**Fluorescence Quantum Yield of Semiconductor Nanocrystals.** Soluble derivatives of semiconductor nanocrystals are receiving increasing attention because of their potential use as very bright, versatile fluorescent probes in biological systems.<sup>18,19</sup> One notable physical characteristic of these particles is their highly temperature-dependent fluorescence quantum yield.<sup>20–22</sup> Figure 3 shows the relative fluorescence yield of 8 nm diameter CdSe nanocrystals<sup>23</sup> arrayed into 36 parallel channels with a temperature gradient from 10 to 80 °C. The

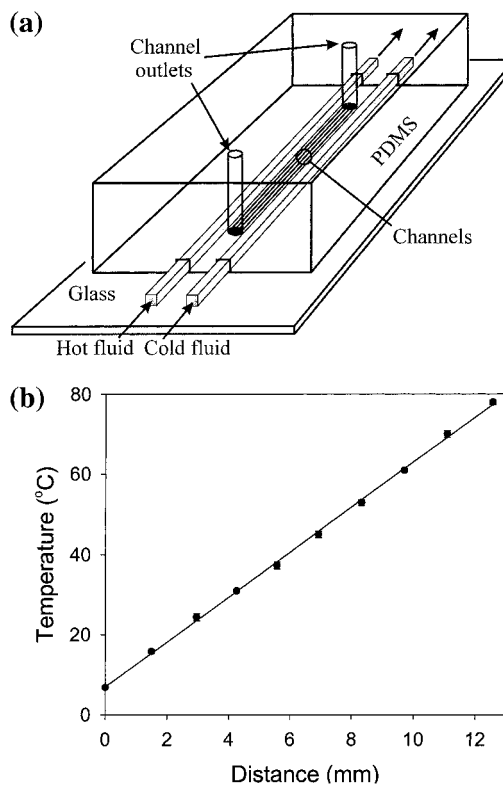


**Figure 2.** (a) Schematic diagram of a device with an on-chip linear temperature gradient. (b) A plot of temperature vs position of the temperature gradient device.

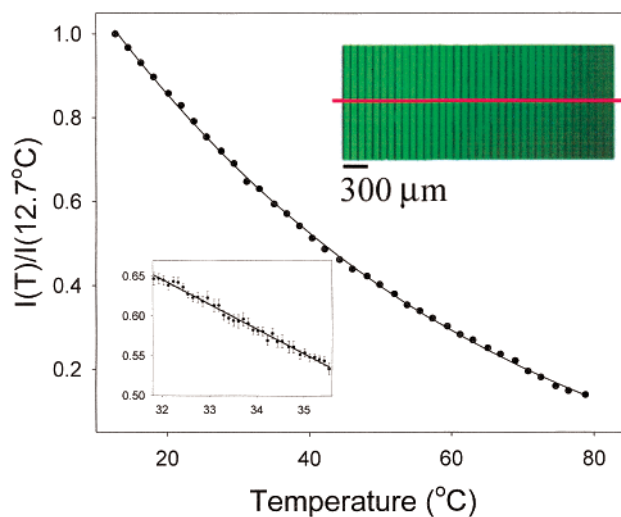


**Figure 3.** A plot of fluorescence data of cadmium selenide nanocrystals in a pH 7.3, 10 mM phosphate buffer solution arrayed over a temperature gradient from 10 to 80 °C. The particles were excited at 470 nm, and emission was measured at 540 nm. The data were taken with an Eclipse 800 fluorescence microscope (Nikon). The variation in temperature across each of the 36 microchannels (cross section for each channel: 80  $\mu\text{m} \times 7 \mu\text{m}$ ) was less than 1.2 °C per microchannel. The upper right-hand inset is the fluorescence image of this experiment. The lower left inset is a plot of data for the identical experiment run over a temperature range from 31.8 to 35.5 °C. The same temperature dependence was noted when channels as big as 250  $\times 7 \mu\text{m}$  and as small as 20  $\times 7 \mu\text{m}$  were used.

quantum yield varied by nearly an order of magnitude over this range and was somewhat nonlinear. On the other hand, an

(17) The use of many parallel channels rather than a single wide one prevents convective mixing in the device and also affords structural stability.

(18) Bruchez, M., Jr.; Moronne, M.; Gin, P.; Weiss, S.; Alivisatos, A. P. *Science* **1998**, *281*, 2013–2018.

(19) Chan, W. C. W.; Nie, S. M. *Science* **1998**, *281*, 2016–2018.

(20) Benisty, H.; Sotomayor Torres, C. M.; Weisbuch, C. *Phys. Rev. B* **1991**, *44*, 10945–10948.

(21) Bawendi, M. G.; Carroll, P. J.; Wilson, W. L.; Brus, L. E. *J. Chem. Phys.* **1992**, *96*, 946–954.

(22) Nirmal, M.; Murray, C. B.; Bawendi, M. G. *Phys. Rev. B* **1994**, *50*, 2293–2300.

(23) CdSe nanocrystals were surrounded by epitaxially grown zinc sulfide shells. This outer layer was capped with a silica coating and then derivatized with sulfhydryl activated PEG groups through siloxane bonds.

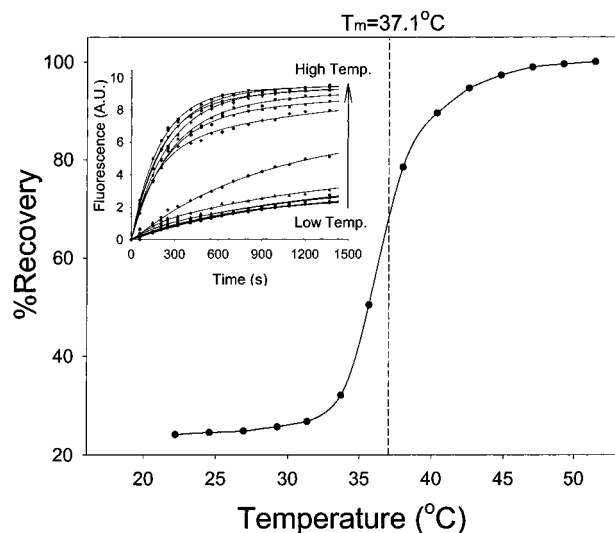


**Figure 4.** Plot of the percent recovery of fluorescence in a lipid bilayer after 1379 s for 14 parallel regions held at different temperatures using the fluorescence recovery after photobleaching technique. The inset shows the recovery curves as a function of time. The line fits shown for this data are to single exponentials.

approximately linear dependence was observed when the experiment was performed over a sufficiently small range (Figure 3, lower left inset). In this case, the experiment was performed with a temperature gradient from 31.8 to 35.5 °C, a separation of roughly 0.1 °C per data point. Obtaining data from even shallower temperature gradients should be possible so long as the heating and cooling elements employed are sufficiently stabilized against thermal drift.

**Phase Transition Measurement in a Phospholipid Membrane.** The ability to determine a phase transition temperature was demonstrated by measuring the main gel to liquid crystalline phase transition temperature for planar supported DPPC bilayers. The lipid membranes consisted of 99 mol % DPPC, a zwitterionic phospholipid with two 16-carbon chains, and 1 mol % of a fluorophore conjugated lipid, NBD-DPPE. Lipid bilayers were coated on the inside walls and floors of an array of 14 microchannels by the vesicle fusion method.<sup>24</sup> The channels were situated in a temperature gradient from 22 to 51 °C, and a line was then bleached simultaneously across the channels at time  $t = 0$ . Because lipid bilayers are liquid crystals, the individual molecular components were constantly mixing in two dimensions in the fluid phase, but mixing far more slowly in the gel phase. As a consequence, photooxidized NBD probes in the photobleached regions were replaced at different rates by fresh probes from the surrounding bilayer regions in the gel and liquid crystalline phases. This caused varying rates of fluorescence recovery in the initially darkened regions in each channel (inset, Figure 4). The percentage of recovery of each region after 1379 s is plotted on the main curve in Figure 4. While little more than 20% recovery was achieved by this point in time when the temperature was below 32 °C, the value approached 100% above 45 °C.<sup>25</sup> The midpoint of the phase transition was near 37 °C, in agreement with literature values.<sup>26,27</sup>

(24) Yang, T.; Jung, S. Y.; Mao, H.; Cremer, P. S. *Anal. Chem.* **2001**, *73*, 165–169.

(25) It should be noted that the fluorescence yield of NBD fluorophores varies somewhat as a function of temperature. The percent recovery, therefore, is plotted as a fraction of the total fluorescence obtained in each region before photobleaching.

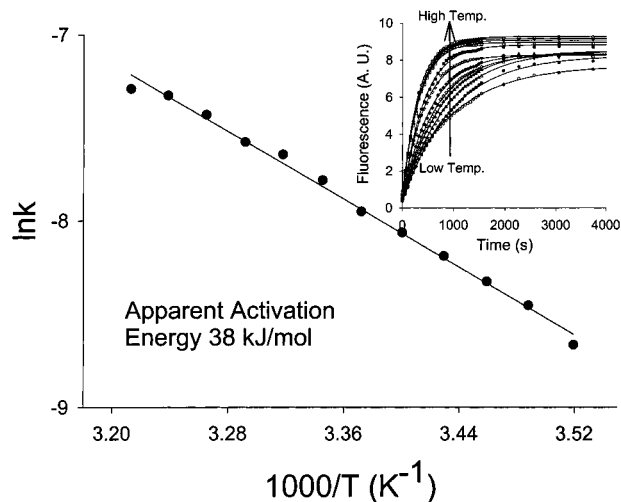


**Figure 5.** An Arrhenius plot of the dephosphorylation of 4-methylumbelliferyl phosphate to 7-hydroxy-4-methylcoumarin catalyzed by alkaline phosphatase immobilized in an array of 14 microchannels. The initial concentration of the substrate was 3.41 mM in a pH 9.8 sodium carbonate buffer with a total ionic strength of 150 mM. The inset shows the reaction curves which were fitted by single exponentials of the form  $F = F_0 + b(1 - e^{-kt})$  to obtain the values of  $k$ .

**Activation Energy of a Phosphatase Enzyme.** The Arrhenius equation can be used to determine the activation energy,  $E_a$ , for a chemical or biochemical reaction (eq 3):

$$\ln k = \ln A - \frac{E_a}{RT} \quad (3)$$

where  $k$  is now the rate constant of the reaction,  $A$  is a preexponential factor,  $T$  is the temperature, and  $R = 8.314$  J/K mol is the gas constant. By running the reaction at several different temperatures and plotting  $\ln k$  versus  $1/T$ , one finds a line with a slope of  $-E_a/R$  and its y-intercept at  $\ln A$ . Here we determined  $E_a$  for the dephosphorylation of the nonfluorescent substrate, 4-methylumbelliferyl phosphate, to the highly fluorescent product, 7-hydroxy-4-methylcoumarin. The dephosphorylation was carried out by the enzyme, alkaline phosphatase, which was immobilized on the walls and floors of the phospholipid bilayer coated microchannels by covalently linking it to the protein streptavidin and presenting 3 mol % biotinylated lipids<sup>28</sup> in the membrane. Substrate was infused into the linear array of microchannels, mechanical valves<sup>29,30</sup> at both ends were then shut, and the rate of product formation was directly monitored by fluorescence microscopy. Figure 5 shows the results for a temperature gradient from 9 to 38 °C in 14 separate channels. The apparent activation energy of the reaction in this case was 38 kJ/mol, which is in good agreement with dephosphorylation rates of similar substrates.<sup>31,32</sup>

## Discussion

In the examples presented above, data acquisition times were cut down by at least one order of magnitude in comparison

(26) Tamm, L. K.; McConnell, H. M. *Biophys. J.* **1985**, *47*, 105–113.

(27) Yang, J.; Appleyard, J. *J. Phys. Chem. B* **2000**, *104*, 8097–8100.

(28) Biotin is a small molecule ligand, which binds very tightly to the 66 k dalton protein, streptavidin.

(29) Mao, H.; Yang, T.; Cremer, P. S. *Anal. Chem.* **2002**, *74*, 379–385.

(30) Unger, M. A.; Chou, H. P.; Thorsen, T.; Scherer, A.; Quake, S. R. *Science* **2000**, *288*, 113–116.

(31) Craig, D. B.; Arriaga, E. A.; Wong, J. C. Y.; Lu, H.; Dovichi, N. J. *J. Am. Chem. Soc.* **1996**, *118*, 5245–5253.

(32) Goodwin, M. G.; Avezoux, A.; Dales, S. L.; Anthony, C. *Biochem. J.* **1996**, *319*, 839–842.

with corresponding sequential measurements. Furthermore, the simple methodology laid out here for generating linear temperature gradients inside microfluidic devices should afford new opportunities to exploit combinatorial strategies in a wide variety of systems. One simple example would be to exploit linear temperature gradients for one-shot measurements of DNA melting curves. More sophisticated devices for multivariable studies of protein crystallization could be envisioned using a series of valves to create sealed wells. In this case, temperature could be varied along one direction, while concentration or pH is varied along another. This would enable hundreds or even thousands of protein solutions to be monitored simultaneously with very rapid sample setup and only minimal material requirements. Obtaining large data sets for phase transitions should make it possible to construct phase diagrams from a single measurement. In addition, adding temperature as a variable to combinatorial methodologies should open up new vistas in materials science such as the rapid testing of novel physical properties or in the field of multiplexed sensor arrays<sup>33</sup> for developing electronic noses and tongues.

## Experimental Section

**Materials.** Phospholipid vesicles were formed from mixtures of 1,2-dilauroyl-*sn*-glycero-3-phosphocholine (DLPC) and *N*-Biotinyl-Cap-PE (16:0) in the enzyme reactions as well as 1,2-dipalmitoyl-*sn*-glycero-3-phosphocholine (DPPC) and 1,2-dipalmitoyl-*sn*-glycero-3-phosphoethanolamine-*N*-(7-nitro-2-1,3-benzoxadiazol-4-yl) (NBD-DPPE) in the phase transition measurements (Avanti Polar Lipids, Inc, Alabaster, AL). Streptavidin-conjugated alkaline phosphatase (1:1 stoichiometry) and 4-methylumbelliferyl phosphate were purchased from Molecular Probes (Eugene, OR). Cleaning solution (7X) came from ICN Bio-medicals, Inc. Photoresist Microposit S 1813 and Microposit Developer were purchased from Shipley Co. (Marlborough, MA). Brass tubes came from K & S Engineering (Chicago, IL), and syringe needles came from Becton Dickinson & Co. (Franklin Lakes, NJ).

**Preparation of Small Unilamellar Vesicles.** SUVs formed from phospholipids, fluorescently labeled phospholipids, and biotinylated phospholipid mixtures were prepared using the Barenholz method.<sup>34</sup> Briefly, lipids dissolved in chloroform were mixed together to the desired mole ratio. The solvent was evaporated in a stream of dry nitrogen followed by vacuum evaporation for an additional 4 h. The dried lipids were reconstituted in phosphate buffer (pH 7.4, ionic strength 150 mM) and sonicated with a titanium tip to form SUV solutions. The samples were centrifuged at 38 000 rpm (94 500g) for 30 min, and then the supernatant was centrifuged again at 52 000 rpm (176 900g) for 3 h using a Beckman Ultracentrifuge L7 with a Ti-75 rotor.

- (33) Albert, K. J.; Lewis, N. S.; Schauer, C. L.; Sotzing, G. A.; Stitzel, S. E.; Vaid, T. P.; Walt, D. R. *Chem. Rev.* **2000**, *100*, 2592–2626.  
(34) Barenholz, Y.; Gibbes, D.; Litman, B.; Goll, J.; Thompson, T.; Carlson, F. *Biochemistry* **1977**, *16*, 2806–2810.

**Fabrication of a Linear Temperature Gradient Device.** The device (Figure 2a) used in these experiments was formed by soft lithographic techniques.<sup>35</sup> First, poly(dimethylsiloxane) (PDMS) (Dow Corning Sylgard Silicone Elastomer-184, Krayden, Inc.) channels were formed by replica molding on a photoresist patterned surface onto which two 1/16-inch wide hollow square brass tubes had been laid in parallel and raised on 200  $\mu\text{m}$  thick stints. The PDMS surface was then rendered hydrophilic by oxygen plasma treatment (PDC-32G plasma cleaner, Harrick Scientific, Ossining, NY) and bonded to a glass coverslip. Glass coverslips, which served as floors of the microchannels, were cleaned in hot surfactant solution (ICN  $\times 7$  detergent, Costa Mesa, CA), rinsed at least 20 times in purified water from a NANOpure Ultrapure Water System, and then baked in a kiln at 400  $^{\circ}\text{C}$  for 4 h before use. Sample materials in aqueous solution were flowed in through the inlet port using a Harvard PHD 2000 syringe pump (Harvard Apparatus, Holliston, MA), while hot and cold fluids were introduced through the brass tubing using standard waterbath circulators (Fisher Scientific, Pittsburgh, PA).

The temperature gradient in Figure 2b was determined in a microfluidic device with eight channels lying between the parallel heating and cooling tubes, which were separated by 12.6 mm. Using a syringe needle, 10 holes were drilled above the eight channels and two metal tubes. The holes were formed in a line perpendicular to the brass tubes. A thermocouple (Omega Engineering, Inc., Stamford, CT) was used to probe the temperature at each location from which a plot of temperature versus position was made. In subsequent devices, temperature measurements were made only over the two brass tubes and interpolated for the intervening channels.

A temperature distribution from 8 to 80  $^{\circ}\text{C}$  is shown in Figure 2b. It should be noted that the viscosity of water is about a factor of 4 greater at 8  $^{\circ}\text{C}$  than it is at 80  $^{\circ}\text{C}$ . This means that the flow rate through the hottest channel was roughly 4 times faster than that through the coldest channel. Since steady state temperatures are achieved extremely rapidly in microfluidic systems due to their very low heat capacity, this had no noticeable effect on the linear temperature distribution.<sup>36</sup>

**Acknowledgment.** This work was supported by ARO (DAAD19-01-1-0346), an ONR-YIP Award (N00014-00-1-0664), the Texas Advanced Technology Program (grant 010366-0181-1999), and a Nontenured Faculty Award from 3M Corporation. CdSe nanocrystals were kindly provided by Wolfgang Parak and Paul Alivisatos at UC Berkeley. The authors wish to acknowledge Hagan Bayley for useful discussions in the preparation of this manuscript.

JA017625X

- (35) Xia, Y.; Whitesides, G. M. *Angew. Chem., Int. Ed.* **1998**, *37*, 550–575.  
(36) Lowe, H.; Ehrfeld, W. *Electrochim. Acta* **1999**, *44*, 3679–3689.  
(37) Kopp, M. U.; de Mello, A.; Manz, A. *Science* **1998**, *280*, 1046–1048.  
(38) Lagally, E. T.; Medintz, I.; Mathies, R. A. *Anal. Chem.* **2001**, *73*, 565–570.  
(39) Khandurina, J.; McKnight, T. E.; Jacobson, S. C.; Waters, L. C.; Foote, R. S.; Ramsey, J. M. *Anal. Chem.* **2000**, *72*, 2995–3000.  
(40) Burns, M. A.; Mastrangelo, C. H.; Sammarco, T. S.; Man, F. P.; Webster, J. R.; Johnson, B. N.; Foerster, B.; Jones, D.; Fields, Y.; Kaiser, A. R.; Burke, D. T. *Proc. Natl. Acad. Sci. U.S.A.* **1996**, *93*, 5556–5561.  
(41) Kataoka, D. E.; Troian, S. M. *Nature* **1999**, *402*, 794–797.  
(42) Ross, D.; Gaitan, M.; Locascio, L. E. *Anal. Chem.* **2001**, *73*, 4117–4123.